A Modular Variable Temperature FT-IMS Instrument Optimized for Gas-phase Ion Chemistry Applications

Authors: Haley M. Schramm, Elvin R. Cabrera, Cullen Greer, Brian H. Clowers*

Department of Chemistry, Washington State University, Pullman, WA 99163, USA

* Corresponding Author: brian.clowers@wsu.edu

Abstract

The latest iteration of modular, open-source rolled ion mobility spectrometers was characterized and tailored for heated ion chemistry experiments. Because the nature of ion-neutral interactions is innately linked to the temperature of the drift cell, heated IMS experiments explicitly probe the fundamental characteristics of these collisions. While classic mobility experiments examine ions through inert buffer gasses, doping the drift cell with reactive vapor enables desolvated chemical reactions to be studied. By using materials with minimal outgassing and ensuring the isolation of the drift tube from the surrounding ambient conditions, an open-source drift cell outfitted with heating components enables investigations of chemical reactions as a function of temperature. We show here that elevated temperatures facilitate an increase in deuterium incorporation and allow for hydrogen/deuterium exchanges otherwise unattainable under ambient conditions. While the initial fast exchanges get faster as temperature is increased, the slow rate which rises from the kinetic nonlinearity though to be attributed to ion-neutral clustering, remains constant with no change in mobility shifts. Additionally, we show the analytical merit of multiplexing mobility data by comparing the performance of traditional signal-averaging and FT-IMS modes.

Keywords: Ion mobility spectrometry; hydrogen-deuterium exchange; ion chemistry

Introduction

The versatility of ion mobility spectrometry has allowed mobility separations to become routine in the areas of trace detection of narcotics and chemical warfare agents, fundamental gas phase ion chemistry, and structural studies of biopolymers.[1–4] Furthermore, due to its compact size and the ability to operate at atmospheric pressure, an ion mobility spectrometer (IMS) may be deployed in a variety of environments as a standalone gas-phase separation technique. However, in research spaces, the coupling of mobility instrumentation to mass spectrometers has significantly increased the amount of structural information gained and broadened the technique's usage due to the complementary nature of the mobility and mass domains.

While mobility instrumentation is quite varied in separation schemes and form factors, the most simple to implement is drift tube ion mobility. In addition to its simplicity, the separation can be performed at atmospheric pressures, eliminating the need for vacuum equipment, which lowers the required footprint and overall cost to run. Several iterations of drift tubes have been developed all while improving separation capabilities, cost, and lab footprint with minimal post-processing required.[5] A promising design that uses flexible printed circuit boards (PCB) has been shown to achieve resolutions greater than 80 while weighing less than 10 g.[5–7] This design was compared to a traditional stacked ring tube with the same specifications,[7] and while the resolution of the stacked ring tube was consistently higher than the flexible system (i.e., FlexIMS), the FlexIMS tube excelled with respect to precision.

The FlexIMS used in that effort was modified in the present work and consists of a series of gold-plated electrodes on polyimide, which are quite robust at elevated temperatures. In this respect, few modifications are needed to conduct the heated experiment in contrast to the traditional stacked ring designs assembled in our lab. In the pioneering work using this concept, Smith *et al.* surrounded a flexible set of electrodes with polyimide-insulated heated pads to reach over 100

°C.[6] Although an atmospheric pressure drift tube system is commercially available (Excellims MA3100), an open-source and easily customizable instrument designed with gas-phase ion chemistry applications in mind warrants further developments.

Temperature is an essential parameter in calculating accurate mobilities from the arrival time distributions.[8] Altering the temperature has been shown to affect the separation capacity for a given instrument/analyte system and change the results in downstream calculations of mobility coefficients and ion-neutral collision cross sections (CCS).[9,10] By changing the temperature of the ions, fundamental effects on the ion-neutral collisions manifest in the temperature dependence of the ion-neutral collision integral.[10] Additionally, by changing the temperature to realize analytical gains in the separation capacity for a given set of analytes, it has been shown that the optimum operating temperature for a specific IMS experiment is not unanimous.[9]

Expanding on this point, Tabrizchi showed that while, in ion mobility, the resolution is expected to be temperature dependent, the separation factor should be temperature independent since drift times for two given ions should vary at the same rate.[9] Experimentally, however, some chemical systems show unique separation factors as the temperature is changed. To explain this phenomenon, the effects on the interactions of the neutral molecules with the analyte ions must be taken into account. At lower temperatures, the effects of neutral solvent molecules interact more readily with the ions, changing the effective identities within the ion population. The neutral molecules here refer to the unintentionally introduced reactive vapors that may persist in the IMS device, such as impurities in the drift gas or humidity.[11] Transient ion-neutral clusters that may form during the mobility analysis in various combinations can change the identity of the sampled ions, effectively sampling the vapor association equilibria rather than bare ion motion. As the temperature is increased and clustering is reduced or eliminated, the data more accurately represents the mobility of the bare ion. While the reduced mobility value corrects for temperature using the first approximation equations for K_0, these nuanced ion-neutral interactions are not

captured. Instead, they illustrate how temperature can be used to alter the separation capabilities of a drift cell using experimental parameters.

Similarly, it has been shown that introducing a reactive modifier into the drift gas can improve the separation capacity of a drift tube due to chemically selective ion-neutral clustering.[12,13] For example, the peaks for dimethyl methyl phosphonate and methyl phosphonic acid are unresolved through neat nitrogen but are fully resolved when 2-propanol is doped into the main drift gas at just 20 μL/hr. Similar observations of transient vapor clustering were seen with a suite of amino acids, and when using a deuterated vapor modifier, simultaneous hydrogen/deuterium exchange (HDX) was observed.[14] These applications to gas-phase ion chemistry allow for added dimensions in structural studies with minimal alterations to an existing instrument.

This report presents modifications of the previous iteration of the flexible DT-IMS to include a gas-tight construction and the capacity to realize variable temperature IM-MS studies. First, the stand-alone, single-gate system was characterized with tetraalkylammonium salts before the addition of a second gate and mounted on the front of the mass spectrometer, highlighting one of the benefits of modular assembly. Here, we explicitly evaluate the improvements in performance using FT-IM-MS over signal averaging on mobility data. Then, variable temperature mobility experiments were performed on a mixture of analytes to observe the effects of temperature on mobility. By modifying the drift gas with deuterated vapor, we also show the capabilities for manipulating the temperature of the drift tube when utilized as a reaction vessel to capture temperature-dependent aspects of hydrogen-deuterium exchange.

Experimental

Tube Assembly

The flexible polyimide PCB sheets were rolled and inserted into a custom-built PEEK (polyether ether ketone) housing with an opening on the top to allow for the sheet to curl out. Instead of directly attaching a resistor chain onto the flexible PCB at the opening, it was soldered to an asymmetrical topboard design that extends beyond the housing, where the electrode chain is separate from the heating elements. The separation from the heating elements and resistor chain was important to ensure that minimal variability was introduced into the generated electric field when operating under variable temperatures. Once the polyimide sheet is rolled and soldered to the top board, the top boards are screwed to the PEEK support chamber which seals with a Viton o-ring. A small amount of vacuum-compatible epoxy (i.e., Torr-Seal) was dabbed where the sheet overlays to keep the rolled polyimide sheet cylindrical and flush with the PEEK housing.

A total of three sections were assembled: two 10.14 cm sections used as the desolvation or drift region and one 25 mm section positioned after the second gate for multiplexing experiments. The ending section was made to host the drift gas inlet to minimize the space without an electric field before the entrance to the mass spectrometer. The designs for the respective parts are available via the following repository: https://github.com/bhclowers. The annotated tube assemblies are shown in Figure 1. A 3D-printed prototype is shown in Figure S1, and images of the operational heated system can be seen in Figure S2.

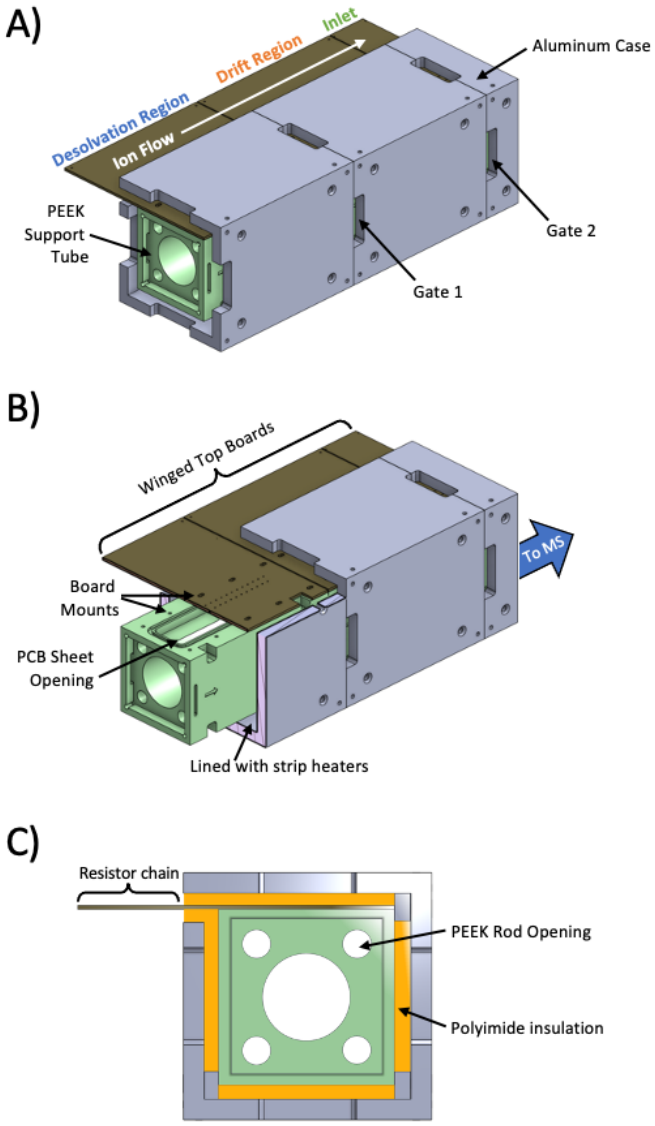

Figure 1: Instrumental schematics. A) The PEEK rolled PCB support structure (green) and aluminum casing (gray). The modular design can be operated as a stand-alone system with just the desolvation and drift regions with a Faraday plate detector or with the addition of a second gate and the inlet section. B) The flexible PCB electrodes are soldered to a top board that extends beyond the heated aluminum case. The support tube has an opening at the top so that the rolled sheet/top board assembly sits flush with the top of the support tube with a space for an O-ring to ensure separation from the atmosphere. C) The grounded aluminum case was lined with strip heaters and insulated in the extra spaces with a polyimide sheet. The resistor chain that creates the electric field extends past all the heating elements. The different modules of the instrument were aligned by PEEK rods through the holes in the support tube and held tightly together using machined aluminum brackets on the outside of the heated case.

Heating Components

A grounded aluminum case for each of the modular sections was machined to fit around the drift tube with just enough room for heaters and insulation between the nested tube on all four sides. The tube was then electrically and thermally insulated with polyimide foam sheet sections (McMaster-Carr #8723K41) and surrounded by the case lined with resistive strip heaters. The strip heaters were placed on each wall of the case and controlled using a NOVUS 1050 temperature controller capable of executing ramp and soak functions. This entire assembly was wrapped in sections of ceramic fire blanket and secured using polyimide tape to reach up to 95 °C.

To ensure effective heating of the drift gas before entry into the drift cell, an Omega CSi32 benchtop controller heated the gas mixer block. Images of the gas mixer can be found in Figure S3. A thermocouple placed between the output of the gas mixer block and the inlet of the drift tube ensured that there was no temperature drop from the mixer to the drift tube. The gas mixer temperature was set to 5 °C above the IMS, and the measured temperature of the gas inlet was always between those two temperatures. The temperature of the drift gas was measured before data collection after allowing the instrument to equilibrate overnight at that temperature and the drift gas flow rate to equilibrate for at least an hour. The overnight equilibration was not necessary to achieve a stable temperature but was convenient for sampling and processing data. This was to ensure the temperature of the drift tube remained constant over the entire time of data collection, which was checked afterward. As reported previously, a small temperature gradient at the front of the tube was observed due to the opening entrance. While not significant for the characterization of the tube in acquiring accurate and precise mobilities, this would have implications for ion chemistry experiments. To correct for this experimental reality, an additional unheated PEEK front cap with a small opening for the ESI source was attached to the front of the IMS. This served to correct the temperature gradient with no observable effects on ionization.

Sample Preparation and Electrospray Ionization Parameters

Tetraalkylammonium (TXA) salts: tetrapentylammonium bromide (T5A), tetrahexylammonium bromide (T6A), tetraheptylammonium bromide (T7A), tetraoctylammonium bromide (T8A), tetrakisdecylammonium bromide (T10A), and tetradodecylammonium bromide (T12A), as well as phenylalanine, methionine, cocaine, and bradykinin, were purchased from Sigma-Aldrich. Stock solutions of the amino acids and bradykinin were prepared by dissolving in DI H_2O and stored at 5 °C. All TXAs were diluted to 1 μM in acetonitrile for analysis. To realize variable temperature kinetic effects, the following analytes and concentrations were used: phenylalanine 30 μM, methionine 60 μM, cocaine 2 μM, and bradykinin 20 μM in methanol and 0.1% formic acid. Working solutions were electrosprayed at 3 μL/min into the IMS using a 75 μm ID glass capillary using an applied potential of 2.2 kV above the entrance potential of the IMS.

Signal Averaged Standalone IMS Characterization

Mobility spectra were recorded as described previously using an electrically floating gate pulser. Ion packets were pulsed into the drift region as controlled by a Digilent Analog Discovery 2 unit (Digilent Pullman, WA).[7] The mobility signals were detected by a Faraday plate constructed in-house.[15] Five gate pulse widths from 100 to 500 μs were evaluated.[16,17] This range yielded results as expected, and was used as a check of instrument robustness. The countercurrent drift gas was nitrogen at 0.4 L/min. At each gate pulse width, three different voltages were applied to the drift tube, and mobility spectra were collected. Each condition was repeated 3 times for a total of 45 measurements. One thousand mobility spectra were averaged for each measurement.

Multiplexed FT-IM-MS

While the hybridization between ion mobility and mass spectrometers has proved essential to many applications, practical challenges in instrument development still remain. The duty cycle mismatch, particularly between drift tube IMS and trapping mass spectrometers, has hindered usage when the mass scans samples at a rate too slow to embed mobility data. While initial efforts, including a second ion gate, accounted for this discrepancy, experimental time scales increased significantly, detracting from the original advantage of fast analyses, especially when recording mobilities for ions that are dispersed in a wide *m/z* range.[18] However, Fourier-based multiplexing has enabled the mobility information to be encoded within the mass spectrometry data. This approach solves the duty cycle mismatch without increasing experimental times while also increasing ion throughput and, in turn, the signal-to-noise ratio. Efforts to optimize the Fourier transform ion mobility-mass spectrometry (FT-IM-MS) approach have been explored recently with considerable .[19–24]

Transient ion signals were extracted from the mass spectrum data of an LTQ XL (Thermo Fischer Scientific, Thousand Oaks, CA) and subsequently, Fourier transformed as described previously.[20] The resulting frequency-domain spectrum was then converted to a drift time spectrum by dividing the frequency (Hz) values by the frequency sweep rate (Hz/s). The synchronized gates were pulsed using a frequency sweep from 5 Hz to 7505 Hz in 1000 scans each 100 ms long as recommended by published work.[24] The countercurrent drift gas was N_2 at 2.1 L/min to account for the gas that is drawn into the inlet of the mass spectrometer.

Results and Discussion

Signal averaging versus Multiplexing

The IMS was first tested as a standalone mobility cell with a TXA mixture. The calculated reduced mobility coefficients for each of the TXA ions were in acceptable agreement with the literature results.[24,25] Once it was confirmed that the drift cell yielded accurate and precise mobilities when operated with the traditional signal averaging methodology, the spectrometer was outfitted with a second gating mechanism and a mount that clamps onto the inlet of the mass spectrometer. Since the system is modular, the addition of a second gate is easily installed by adding the inlet section along the PEEK rods with an electrical connection on the winged top boards. As explained previously, mobility spectra were obtained with the same ESI solution using a Fourier-based multiplexing approach.[20] All mobility values fall within a 4% error margin.[24,25] This comparison highlights not only the reproducibility when using comparable IMS instrumentation but also that there is no effect on the accuracy or precision of the IMS data whether a signal averaging or multiplexing approach is used in the case of TXA salts. An additional discussion related to the precision and accuracy of absolute and relative gas-phase ion mobilities is provided in Table S1.

Ion	$^{a}K_0$ Literature [25]	$^{b}K_0$ Literature [24]	K_0 (Signal Averaging)	K_0 (FT Multiplexing)
T5A	1.100 ± 0.012	1.103 ± 0.001	1.110 ± 0.002	1.095 ± 0.004
T6A	0.967 ± 0.006	0.980 ± 0.001	0.986 ± 0.002	0.974 ± 0.004
T7A	0.868 ± 0.003	0.887 ± 0.001	0.892 ± 0.002	0.882 ± 0.003
T8A	0.792 ± 0.008	0.815 ± 0.001	0.818 ± 0.002	0.809 ± 0.003
T10A	0.692 ± 0.006	0.712 ± 0.001	0.713 ± 0.002	0.707 ± 0.003
T12A	0.629 ± 0.006	0.653 ± 0.001	0.652 ± 0.002	0.647 ± 0.002

Table 1: Calculated reduced mobility coefficients for TXA salts. The literature values listed in $^{a}K_0$ were measured with a signal-averaged approach whereas the values in $^{b}K_0$ were collected by multiplexing. The signal-averaged values were obtained as a stand-alone mobility drift cell where the multiplexed data were collected using the FT-IM-MS workflow. In comparing these values, there is no effect on the accuracy of mobility values when using either the signal averaging or multiplexing approach. All associated error values are the standard deviation of four replicates. It is important to note here that these data were taken by three different researchers using three entirely independent home-built instruments via two different modes of data acquisition. While statistically some of the K_0 values fall out of the range of error, the reproducibility of under 4% error for these measurements can be simply attributed to random experimental variability.

While both signal averaging and multiplexing yield accurate and precise mobilities, there are clear analytical advantages to the multiplexing technique seen in Figures 2 and 3. Although the benefits of multiplexing approaches have been reported previously, this explicit data comparison obtained via two operating modes (signal averaging and FT-based multiplexing) on the same instrument has yet to be clearly reported. Additionally, this represents the first open-source instrument design focusing on a variable temperature system where every single part, including files for fabrication, is made available to the public. In the simplest sense presented, here we add further support for multiplexing approaches in drift tube ion mobility spectrometry.

The data acquisition of each method takes about the same amount of experimental time for each replicate. Comparing the spectra obtained from the two methods in Figure 2, the signal-averaged spectra have a lower signal-to-noise ratio and resolving power than the multiplexed spectra. While some effort could be imparted into optimizing a stand-alone system for improved figures of merit, only marginal gains would be expected. This is illustrated clearly by Naylor *et al.* in the differences in the average and maximum resolving powers reported for each TXA salt.[5] The optimal conditions yielding the greatest resolving power for a given instrument are not much larger (and in many cases not statistically different from) the average resolving power for each salt. However, as seen in Figure 3B, appreciable gains in resolving power can be realized with the multiplexing approach, although this does require some alterations to the instrument. More significantly, the signal-to-noise ratios (SNR) are greater by up to two orders of magnitude, as seen in Figure 3A.

The error margins for each acquisition mode stem from different sources: the variability in the signal averaging data for the SNR comes from including multiple GPWs whereas the errors in the multiplexing data are attributed to the varying applied voltage. Here, the applied voltage is the potential applied to the drift cell which changes the electric field strength, however, the lower applied voltages yield a lower ion signal and, in turn, lower the SNR. This discussion highlights a nuanced point - the GPW of the signal averaging method is not a metric used in the multiplexing

approach. In the FT mode, the GPW can be thought of as analogous to the frequency at which the gates are pulsed opened and closed. This is precisely the variable that is changed during the FT multiplexing data acquisition. For this reason, the GPWs were pooled in the SNR calculations for the signal-averaging method. The variability in the signal averaging data for SNR comes from the differences in data obtained from operating at different gate pulse widths, whereas the error in the multiplexing data originates from data collection at different applied voltages, changing the signal intensity.

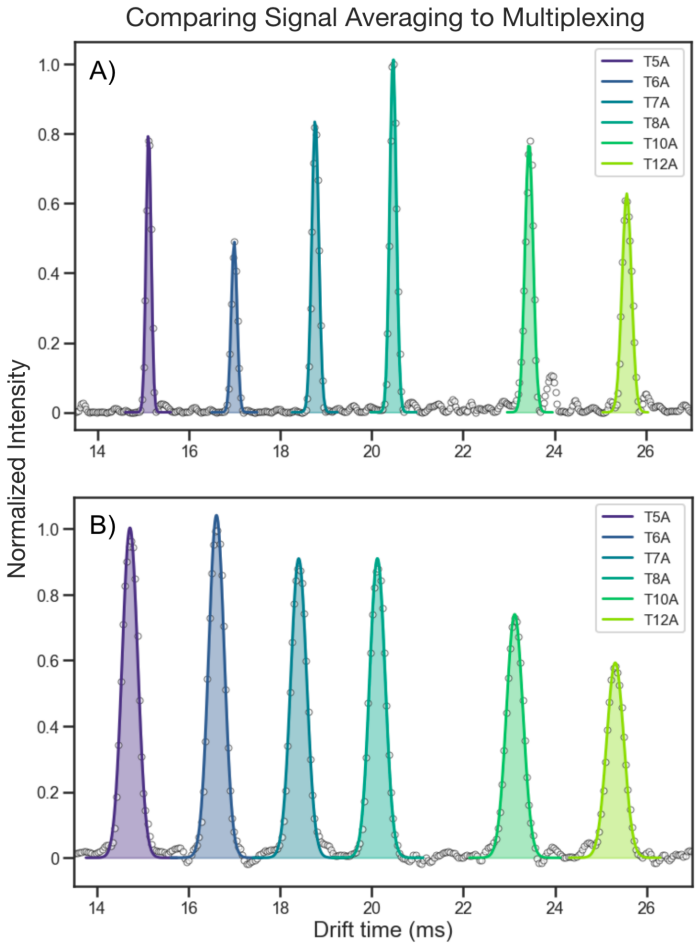

Figure 2: Comparing A) Multiplexed and B) Signal Averaged arrival time distributions (ATDs). The raw data are plotted in gray circles with colored Gaussian fits overlaid. While the multiplexing method allows for mass-selected mobility data, the ATD shown here comes from the entire mass range encompassing T5A to T12A, eliminating any bias in the resulting spectra from the mass selection for resolving power comparisons.

One of the most useful attributes of the modular assembly approach is the accessibility to points of contact for troubleshooting. Within the context of this work, we first checked that the correct mobility values were measured as a stand-alone system with no heating elements. Then, a second gating mechanism was added to the tube along with a mount that clamps onto the mass spectrometer. The mobilities of the TXA mixtures were reevaluated using the multiplexing approach. Finally, the heating elements were added. Even when the case and insulation are on and operational, the user can troubleshoot the mobility components without hindrance, providing ample opportunity to ensure accurate and precise mobility assignments.

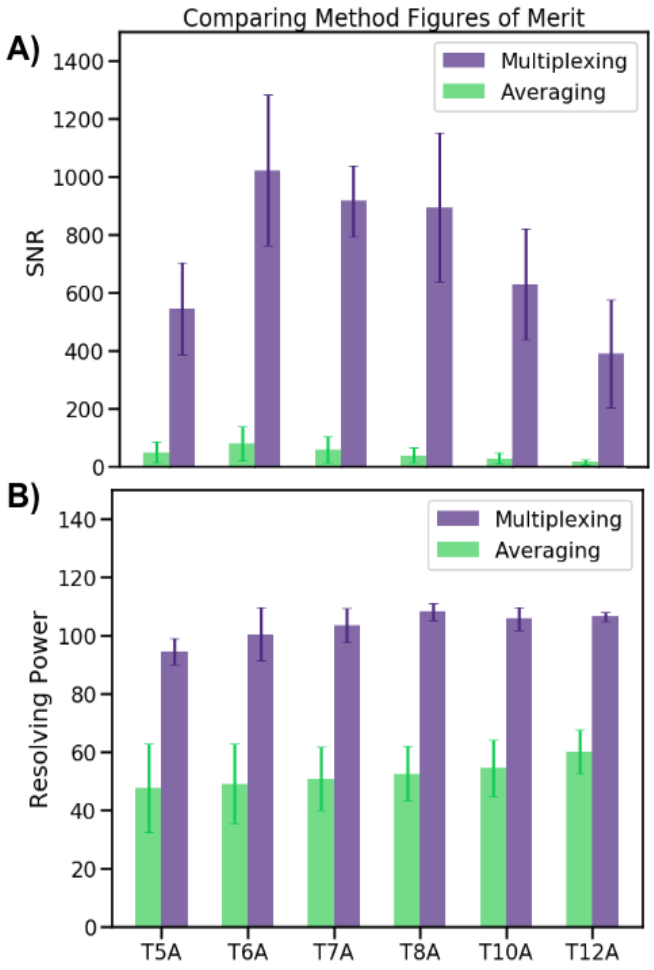

Figure 3: The A) signal-to-noise (SNR) and B) resolving power (RP) comparisons for multiplexing and signal averaging using TXA salts. Both figures of merit for the multiplexed data were calculated post-mass selection. The average resolving powers reported here are in agreement with Naylor *et al.,* highlighting the analytical advantages of multiplexing approaches.[5] The error bars are the standard deviation of 4 replicates.

Temperature Effects on Ion Mobility

It has been shown that arrival time distributions (ATDs) shift at different temperatures depending on the propensity of the ions to retain or attract neutral molecules as a function of charge density, resulting in experimentally specific separation factors.[9] Stated another way, the effective size and mass are dependent on the desolvation characteristics and probability of the ions forming clusters with neutral molecules at different temperatures. Since these parameters are unique to the analyte ions, the highly studied TXA ions were measured over the attainable range of the instrument. In addition to the highly characterized mobility coefficients, the TXAs are ideal standards for these experiments since they have a low propensity for vapor association, minimal expected changes in the cross sections, and exist as positively charged ions in solution, which should reduce the impact of temperature on the measured mobility coefficient.

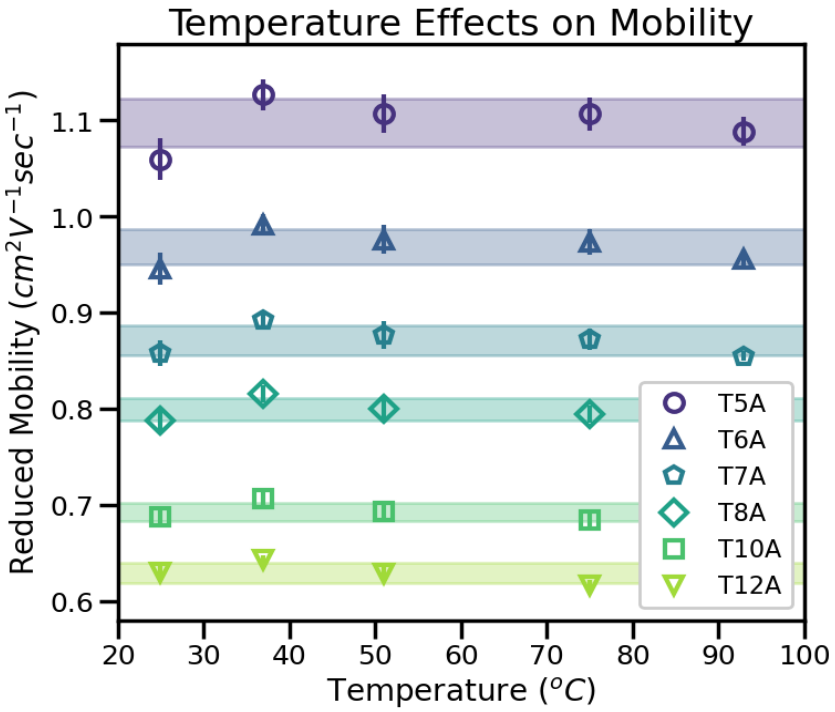

Figure 4: Temperature Effects on Mobility. The reduced mobility (K_0) for select TXA ions as a function of temperature. The error bars on the plotted points represent ±1 standard deviation of 4 replicates at that temperature. At the highest measured temperature (95°C), the signals for T8A, T10A, and T12A were not high enough to extract drift times from the ATD. The colored bands represent one standard deviation about the mean of the mobilities at all temperatures to aid in comparing the variability between temperature points.

Previous work, both in theory and experiment, predicts that drift times will be shorter as the temperature is increased which would consequently increase the mobility coefficient, K.[9] Moving from room temperature (24°C) to 37°C, the reduced mobilities (K_0) of all the TXAs increase slightly. These observed changes illustrate that, even though the K_0 value corrects for temperature variation, there are still effects not captured by the first approximation when calculated K_0 from the drift cell. Stating this another way, the shorter drift times at 37°C when compared to the room temperature measurements are shorter than predicted using the classic relationships between the length, temperature, pressure, and electric field of the drift tube. While the difference is rather small, the mobilities at 37°C would more closely represent the mobilities of the bare ions.

From 37°C to 95°C, the mobilities are rather constant with a minimal gradual decrease. It is important to note that the average K_0 value calculated for each temperature is always less than 4% different from the average K_0 value calculated for the entire temperature range. This observation indicates that after 37°C, the changes in drift time are largely accounted for by the change in drift cell temperature. The slight decreases in the mobilities could be attributed to a minimum in collisional cross section reached, interday variability, or ionization differences. Changes in the ESI process may be likely since the decrease is more pronounced above the boiling point of the solvent, ACN. It is also important to note that at the highest temperature point, the ion signal was lost for T8A, T10A, and T12A. As temperature increases, so does the rate of diffusion. These lower mobility TXA ions spend longer in the drift cell, increasing the effects of diffusion on the peaks. Additionally, the poor solubility of the T8A to T12A ions may also play a role in signal loss. This contention could be tested by repeating these experiments but spraying the analytes from a solvent with a higher boiling point, such as water. Nevertheless, these data illustrate the drift cell suitable for high-fidelity mobility experiments over a wide temperature range.

Variable Temperature Gas-Phase Ion Chemistry Applications

Work done by Valentine and Clemmer first published variable temperature gHDX within a drift cell using cytochrome C.[26] They observed an increase in the extent of deuterium incorporation as the temperature was increased but a decrease in the observed rate. Interestingly, their kinetic data recorded at ambient temperature display a nonlinear trend. This kinetic nonlinearity is ubiquitous in the gHDX data we have taken on an atmospheric pressure drift cell.[14,27] Both experiments also observe changes in the arrival time distributions of the ions as a function of deuterated vapor. This phenomenon has been explained previously by transient ion-neutral clustering. Since we have reason to believe that clustering equilibrium influences these observed gHDX rates, manipulating the temperature can add more data to that idea. As the temperature is increased, the equilibrium shifts towards the bare ion, and experimentally, a smaller change in mobility is observed.[12,28] By manipulating the clustering equilibrium and observing the subsequent effects on gHDX, more insights can be gained into the possible role that vapor association plays in kinetics.

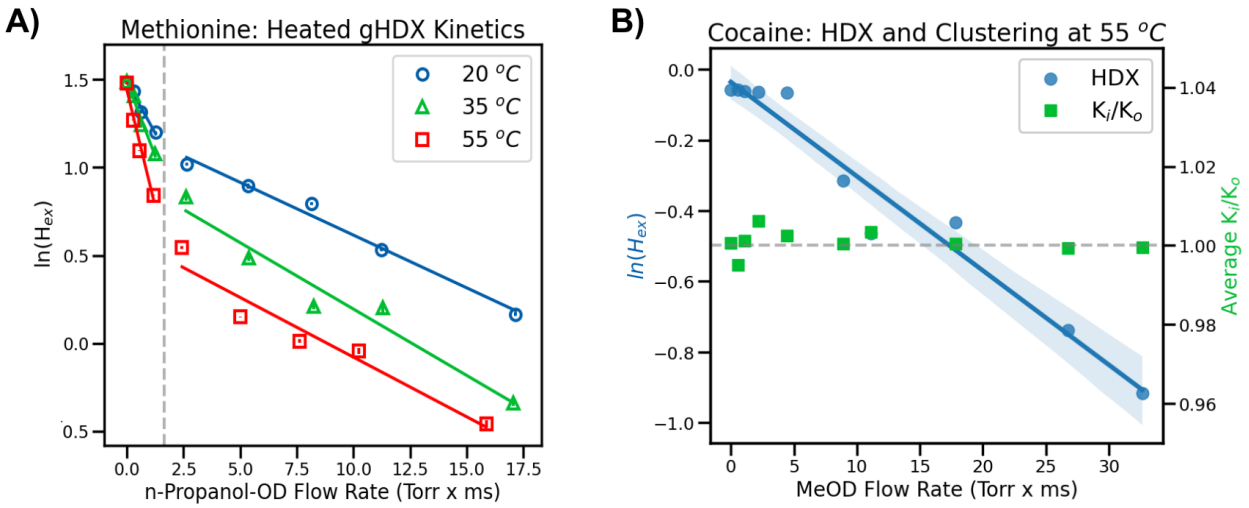

Figure 5: Initial Variable Temperature Ion Chemistry Results. The y-axes labeled "'ln(H_{ex})" come from a pseudo-first order kinetics approach and is a measure of the remaining exchangeable hydrogens. A) The effects of increased temperature on gas-phase hydrogen/deuterium exchange (gHDX) kinetics for methionine with n-propanol-OD. B) While previously used as a control for both clustering and HDX at room temperature, cocaine begins to exchange its singular exchangeable hydrogen at 55 °C with methanol-OD.

The extent of deuterium incorporation increases with temperature, as shown in Figure 5A. The nonlinear behavior in the pseudo-first-order kinetics data reported previously persists as a function of temperature.[14] While the observed fast rate of exchange increases with temperature, the slow exchanges after the breakpoint at higher concentrations of the modifier are comparatively constant. Interestingly, the maximum shifts in mobility remain unchanged over this temperature range. The additional mobility shift axis for these data was excluded from Figure 5A for clarity, but an example can be seen in our previous publication.[14] These observations provide additional evidence that the observed slow rate of exchange is, at least partially, mediated by ion-neutral clustering.

Cocaine has previously been used in room temperature studies as a system suitability check since it did not exchange or form clusters to shift the arrival time distributions of the ions.[14] However, at 55 ^{o}C, cocaine begins to exchange its singular exchangeable hydrogen after 80 µL/hr with methanol-OD as seen in Figure 5B. While increased temperature experiments are expected to enable the detection of systems previously unachievable at ambient conditions, these data are particularly interesting since this is the first observation of an analyte that does exchange but without any detectable changes in mobility. One interpretation of these experimental data is that these types of exchanges occur entirely in the gas phase and do not require transient clustering.

Conclusions and Future Directions

Recent work has shown that clustering affects the observed rates of hydrogen/deuterium exchange (HDX) using select amino acids and peptides.[14,27] This work was built on previous observations that not only can mobility separation factors be tuned using selective ion-neutral clustering, but shifts in the arrival time distributions of ions due to transient ion-neutral clusters can be used to probe energetics of local solvation.[12,13,28] By combining these frameworks to assess thermodynamic parameters of nascent solvation, selective HDX, and molecular dynamics

simulation, a new method for probing conformational dynamics of biopolymers in the gas phase is possible.

Future work with this instrument will be used to calculate the thermodynamics of vapor association from experiments, which will be compared to DFT simulations. In addition, repeating experiments published previously with peptides and proteins using gHDX to infer structural information will aid in comparisons between different pressure regimes.[26,29,30] While the temperature range included as proof of concept for the variable temperature ion chemistry only affected the fast rate of exchange, increasing the accessible temperature to favor the bare ion and observe gHDX without clustering is vital in the interpretation of the ubiquitous gHDX kinetic nonlinearity.

While the development of this instrument was predicated on isotope exchange experiments done within the drift cell, control over the temperature of the IMS is significant for several applications, such as atmospheric particle formation and threat detection. The rolled tube and custom heated case provide an open-source IMS solution that is simply built yet capable of measuring unique chemical kinetics and thermodynamics more challenging to obtain with other methods. For our gHDX work, the control of temperature provided further evidence that clustering influences the kinetic nonlinearity that is commonly observed. Additional work into gHDX at higher temperatures where the shifts in mobility due to clustering are reduced if not eliminated is now possible with this instrument. This work will provide new insights into the nature of gHDX under different microsolvation environments.

Acknowledgments. Support for this work was provided by the NSF (US NSF 2003042) and Redstone Arsenal.

Supporting Information. Photos of the key instrumental components are included in the supporting information along with a discussion of absolute and relative ion mobilities. Additionally, a compressed file archive is included that contains the CAD and PCB files to recreate the described apparatus.

References

(1) Wu, C.; Siems, W. F.; Hill, H. H., Jr. Secondary Electrospray Ionization Ion Mobility Spectrometry/mass Spectrometry of Illicit Drugs. *Anal. Chem.* **2000**, *72* (2), 396–403.
(2) Reid Asbury, G.; Klasmeier, J. rg; Hill, H. H., Jr. Analysis of Explosives Using Electrospray Ionization:ion Mobility Spectrometry (ESI:IMS). *Talanta* **2000**, *50*, 1291–1298.
(3) Theisen, A.; Black, R.; Corinti, D.; Brown, J. M.; Bellina, B.; Barran, P. E. Initial Protein Unfolding Events in Ubiquitin, Cytochrome c and Myoglobin Are Revealed with the Use of 213 Nm UVPD Coupled to IM-MS. *J. Am. Soc. Mass Spectrom.* **2019**, *30* (1), 24–33.
(4) Shi, H.; Pierson, N. A.; Valentine, S. J.; Clemmer, D. E. Conformation Types of Ubiquitin [M+8H]8+ Ions from Water:methanol Solutions: Evidence for the N and A States in Aqueous Solution. *J. Phys. Chem. B* **2012**, *116* (10), 3344–3352.
(5) Naylor, C. N.; Cabrera, E. R.; Clowers, B. H. A Comparison of the Performance of Modular Standalone Do-It-Yourself Ion Mobility Spectrometry Systems. *J. Am. Soc. Mass Spectrom.* **2023**. https://doi.org/10.1021/jasms.2c00308.
(6) Smith, B. L.; Boisdon, C.; Young, I. S.; Praneenararat, T.; Vilaivan, T.; Maher, S. Flexible Drift Tube for High Resolution Ion Mobility Spectrometry (Flex-DT-IMS). *Anal. Chem.* **2020**, *92* (13), 9104–9112.
(7) Chantipmanee, N.; Hauser, P. C. Development of Simple Drift Tube Design for Ion Mobility Spectrometry Based on Flexible Printed Circuit Board Material. *Anal. Chim. Acta* **2021**, *1170*, 338626.
(8) Revercomb, H. E.; Mason, E. A. Theory of Plasma Chromatography/gaseous Electrophoresis. Review. *Anal. Chem.* **1975**, *47* (7), 970–983.
(9) Tabrizchi, M. Temperature Effects on Resolution in Ion Mobility Spectrometry. *Talanta* **2004**, *62* (1), 65–70.
(10) Wyttenbach, T.; Helden, G. von; Batka, J. J.; Carlat, D.; Bowers, M. T. Effect of the Long-Range Potential on Ion Mobility Measurements. *J. Am. Soc. Mass Spectrom.* **1997**, *8* (3), 275–282.
(11) Wolańska, I.; Piwowarski, K.; Budzyńska, E.; Puton, J. Effect of Humidity on the Mobilities of Small Ions in Ion Mobility Spectrometry. *Anal. Chem.* **2023**, *95* (22), 8505–8511.
(12) Kwantwi-Barima, P.; Hogan, C. J., Jr; Clowers, B. H. Probing Gas-Phase-Clustering Thermodynamics with Ion Mobility-Mass Spectrometry: Association Energies of Phenylalanine Ions with Gas-Phase Alcohols. *J. Am. Soc. Mass Spectrom.* **2020**, *31* (9), 1803–1814.
(13) Kwantwi-Barima, P.; Ouyang, H.; Hogan, C. J., Jr; Clowers, B. H. Tuning Mobility Separation Factors of Chemical Warfare Agent Degradation Products via Selective Ion-Neutral Clustering. *Anal. Chem.* **2017**, *89* (22), 12416–12424.
(14) Schramm, H. M.; Tamadate, T.; Hogan, C. J.; Clowers, B. H. Ion-Neutral Clustering Alters Gas-Phase Hydrogen-Deuterium Exchange Rates. *Phys. Chem. Chem. Phys.* **2023**. https://doi.org/10.1039/d2cp04388b.
(15) Reinecke, T.; Clowers, B. H. Implementation of a Flexible, Open-Source Platform for Ion Mobility Spectrometry. *HardwareX* **2018**, *4*, e00030.
(16) Siems, W. F.; Wu, C.; Tarver, E. E.; Hill, H. H., Jr; Larsen, P. R.; McMinn, D. G. Measuring the Resolving Power of Ion Mobility Spectrometers. *Anal. Chem.* **1994**, *66* (23), 4195–4201.
(17) May, J. C.; Dodds, J. N.; Kurulugama, R. T.; Stafford, G. C.; Fjeldsted, J. C.; McLean, J. A. Broadscale Resolving Power Performance of a High Precision Uniform Field Ion Mobility-Mass Spectrometer. *Analyst* **2015**, *140* (20), 6824–6833.
(18) Zucker, S. M.; Lee, S.; Webber, N.; Valentine, S. J.; Reilly, J. P.; Clemmer, D. E. An Ion Mobility/ion Trap/photodissociation Instrument for Characterization of Ion Structure. *J. Am. Soc. Mass Spectrom.* **2011**, *22* (9), 1477–1485.

(19) Knorr, F. J.; Eatherton, R. L.; Siems, W. F.; Hill, H. H., Jr. Fourier Transform Ion Mobility Spectrometry. *Anal. Chem.* **1985**, *57* (2), 402–406.
(20) Morrison, K. A.; Siems, W. F.; Clowers, B. H. Augmenting Ion Trap Mass Spectrometers Using a Frequency Modulated Drift Tube Ion Mobility Spectrometer. *Anal. Chem.* **2016**, *88* (6), 3121–3129.
(21) Sanders, J. D.; Butalewicz, J. P.; Clowers, B. H.; Brodbelt, J. S. Absorption Mode Fourier Transform Ion Mobility Mass Spectrometry Multiplexing Combined with Half-Window Apodization Windows Improves Resolution and Shortens Acquisition Times. *Anal. Chem.* **2021**, *93* (27), 9513–9520.
(22) Butalewicz, J. P.; Sanders, J. D.; Clowers, B. H.; Brodbelt, J. S. Improving Ion Mobility Mass Spectrometry of Proteins through Tristate Gating and Optimization of Multiplexing Parameters. *J. Am. Soc. Mass Spectrom.* **2023**, *34* (1), 101–108.
(23) Cabrera, E. R.; Clowers, B. H. Synchronized Stepped Frequency Modulation for Multiplexed Ion Mobility Measurements. *J. Am. Soc. Mass Spectrom.* **2022**, *33* (3), 557–564.
(24) Cabrera, E. R.; Clowers, B. H. Considerations for Generating Frequency Modulation Waveforms for Fourier Transform-Ion Mobility Experiments. *J. Am. Soc. Mass Spectrom.* **2022**, *33* (10), 1858–1864.
(25) Naylor, C. N.; Reinecke, T.; Clowers, B. H. Assessing the Impact of Drift Gas Polarizability in Polyatomic Ion Mobility Experiments. *Anal. Chem.* **2020**, *92* (6), 4226–4234.
(26) Valentine, S. J.; Clemmer, D. E. Temperature-Dependent H/D Exchange of Compact and Elongated Cytochrome c Ions in the Gas Phase. *J. Am. Soc. Mass Spectrom.* **2002**, *13* (5), 506–517.
(27) Schramm, H. M.; Tamadate, T.; Hogan, C. J.; Clowers, B. H. Evaluation of Hydrogen-Deuterium Exchange during Transient Vapor Binding of MeOD with Model Peptide Systems Angiotensin II and Bradykinin. *J. Phys. Chem. A* **2023**. https://doi.org/10.1021/acs.jpca.3c04608.
(28) Kwantwi-Barima, P.; Hogan, C. J., Jr; Clowers, B. H. Deducing Proton-Bound Heterodimer Association Energies from Shifts in Ion Mobility Arrival Time Distributions. *J. Phys. Chem. A* **2019**, *123* (13), 2957–2965.
(29) Suckau, D.; Shi, Y.; Beu, S. C.; Senko, M. W.; Quinn, J. P.; Wampler, F. M., 3rd; McLafferty, F. W. Coexisting Stable Conformations of Gaseous Protein Ions. *Proc. Natl. Acad. Sci. U. S. A.* **1993**, *90* (3), 790–793.
(30) Valentine, S. J.; Clemmer, D. E. H/D Exchange Levels of Shape-Resolved Cytochrome c Conformers in the Gas Phase. *J. Am. Chem. Soc.* **1997**, *119* (15), 3558–3566.

Supporting Information. Photos with details of the nested ion mobility cell, the heated cell mounted on an LTQ, and the heated gas mixer.

For Table of Contents Only: